

Multiwire Gas Proportional Counters: Decrepit Antiques or Classic Performers?

R. Lewis

Daresbury Laboratory, Warrington WA4 4AD, UK

(Received 6 April 1994; accepted 16 June 1994)

An overview of the operational characteristics of multiwire gas proportional counters is given with particular reference to their use in X-ray diffraction. Their strengths and weaknesses are analysed and it is demonstrated that these devices are able to offer a combination of features that is unique. Some examples of synchrotron radiation experiments performed with gas detectors are used to illustrate their performance, and finally, the current status of development and prospects for the future development of gas detectors are reviewed.

Keywords: detectors; proportional counters; wire chambers.

Introduction

Ever since the birth of dedicated synchrotron radiation sources, there has been a considerable mismatch between the fluxes provided by storage rings and the ability of X-ray detection systems to exploit them. It is, therefore, very often the detection system that limits the final data quality with new third-generation sources only serving to exacerbate the situation. There is no ideal detector which can be used for all synchrotron radiation experiments, and it is increasingly important that the detection system best matched to the requirements of each experiment be chosen from the wide variety of X-ray detection systems available. This paper reviews some of the properties of multiwire gas proportional counters (MWPCs) for X-ray detection and the particular features that they offer the synchrotron radiation experimenter. It is not intended to be a comparative review of all types of X-ray detectors.

The position-sensitive MWPC was developed at CERN during the late 1960s for X-ray and particle detection in high-energy-physics experiments by G. Charpak and co-workers (Charpak, Bouclier, Bressani, Favier & Zupancic, 1968; Charpak, 1970) and since then it has been used in many fields ranging from astronomy to nuclear physics. Within the very wide field of synchrotron radiation research, the experimental technique that has made most use of the MWPC is X-ray diffraction.

Synchrotron radiation detector requirements

In 1991 a European Workshop on X-ray detectors for synchrotron radiation drew up a set of guideline specifications for a suitable detector to exploit the new sources for X-ray diffraction. These are shown in Table 1.

Diffraction patterns have an enormous range of intensities, often covering more than four decades, and so, despite the enormous X-ray fluxes generated by storage rings, the weaker parts of the pattern may contain only a few photons.

Table 1

Guideline specifications for an X-ray detector for diffraction experiments [after Walenta (1992)].

Characteristic	Required specification
Resolution	250 × 250 μm
No. of pixels	1800 × 1800
Total count rate	10 ⁸ s ⁻¹
Local count rate	5 × 10 ⁵ s ⁻¹ mm ⁻²
Dynamic range	> 10 ⁶
Stability/reproducibility	10 ⁻³ –10 ⁻² h ⁻¹
Sensitivity	1 photon pixel ⁻¹
No. of frames	256
No. of cycles	1000
Frame rate	10 ⁵ s ⁻¹
Energy range	2–35 keV
Typical energy	10 keV
Energy resolution, ΔE/E	20%

The detection system should therefore have a response which is linear over the full range of intensities, and also be as sensitive as possible with the minimum of noise.

Sensitivity is a complex parameter which is affected by the absorption efficiency of X-ray photons, the detector noise level (sometimes called the 'fog' level) and the point-spread function (spatial resolution) of the detector. It is quite possible for a detector to have a high efficiency for the absorption of X-ray photons but a rather poor sensitivity owing to a high noise level, *e.g.* X-ray film. Moreover, a detector may be rather more sensitive to certain types of images than to others. X-ray film is more sensitive to images containing sharp peaks than to those containing diffuse features because of its excellent point-spread function but rather poor fog level. The exact signal-to-noise level delivered by a given detector system depends in a complex manner upon the nature of the experiment but, clearly, high detection efficiency and low noise are very desirable characteristics.

It is sometimes thought that a poor detector sensitivity can be compensated for, by taking longer exposures or by

using more intense beams. However, this is not necessarily the case. If the sample is susceptible to radiation damage, as with practically all biological samples, it is crucial to minimize the dose to the sample. The detector must therefore have the highest possible sensitivity. In addition, in dynamic experiments where it is required to follow changes occurring in the image, the sensitivity of the detector has a direct effect upon the achievable time resolution.

X-ray diffraction requires accurate measurements of the intensities and positions of features in the image, in some cases as a function of time. A useful detection system must therefore be able to record this information with the minimum possible distortion. Errors caused by factors such as non-uniformity of response over the active area of the detector and non-linear mapping of photon position, can largely be corrected by performing calibration measurements, always provided that the performance of the system remains stable between calibration and experiment. In experiments such as crystalline diffraction, the need to make accurate intensity measurements of closely spaced peaks demands a good point-spread function whilst time-resolved experiments require detectors that can record a succession of images with the minimum possible dead-time.

The physical size of the detector is important. X-ray beams have finite dimensions and there is little to be gained by having a pixel size much smaller than the size of the beam. Large detectors enable a wide range of scattering angles to be sampled in a single diffraction experiment and also allow the detector to be placed further away from the sample which reduces the background scattering component on the image.

Finally, the practical requirements of day to day use on a beamline also mean that the detectors must be able to operate reliably over periods of weeks.

Detector categories

X-ray detector systems can be grouped into two broad categories, which each have advantages and disadvantages.

Photon-counting detectors

Imaging photon-counting detectors such as the MWPC are essentially digital devices that can distinguish between the presence and absence of a single X-ray at any point on the detection surface. A counter is generally incremented upon the arrival of each photon. This operation obviously requires time, during which at least a portion of the detector becomes insensitive to further photons. This dead-time occurs for every photon and therefore the total amount of dead-time is a function of input flux. At some point the detector will saturate; this defines a maximum input rate and, consequently, the data throughput. However, as each recorded photon is read-out immediately after arrival, there is essentially zero read-out time at the end of a frame. The minimum detectable flux is limited by the dark noise, which is the count rate for zero input flux. In photon-

counting devices it can be made very low and in practice is often swamped by the levels of background radiation such as cosmic rays. The detector noise levels in such a system are by definition less than one photon per pixel, which means that these detectors can operate with close to ideal performance with the output signal-to-noise ratio being mainly limited by photon statistics over the limited operating range of input fluxes.

As each photon is detected individually, photon counting also allows the position, wavelength and arrival time of each individual photon to be recorded, provided that the detection system has been designed to record all such information.

Integrating detectors

In contrast to counting detectors, integrating devices record X-ray intensity by measuring the level of some quantity which changes as a function of X-ray flux. It is an analogue process where the accuracy of an intensity measurement depends upon the noise present during the assessment of the varying quantity. Integrating systems do not electronically count each photon and so can often tolerate very high input fluxes; however, they do have to be read-out at the end of the frame period resulting in a frame-rate-dependent dead-time. Obviously, it is advantageous to make this time as small as possible, but as the read-out speed is increased, so the read-out noise increases. Dark noise in integrating detectors is caused by a combination of the read-out noise and random fluctuations in the quantity being measured. It is often related to temperature, and cooling the detector and/or front-end electronics can help in certain cases. As in photon-counting devices, the dark noise determines the minimum detectable flux, but in this case it is likely to be a function of read-out speed. There is therefore usually a trade-off between time resolution and sensitivity.

At a certain input intensity, the quantity being measured will saturate. This does not set an instantaneous maximum input rate but rather a maximum number of X-rays that can be measured in a pixel before the detector must be read out and the pixels reset. Given a certain input flux therefore, the detector must be read out or replaced sufficiently often to prevent saturation. Since the detector cannot detect X-rays during read-out or replacement, this time sets a limit on the overall data throughput.

Examples of this type of detector are CCDs, TV detectors and image plates.

The multiwire proportional counter

Fundamentals

It is beyond the scope of this article to give a detailed description of the operation of MWPCs. Only an outline is given here and the interested reader is referred to Sauli (1977).

The initial event in the detection of a photon by a gas detector is the absorption of an X-ray by a gas atom or molecule with the emission of a photo or Auger electron. A complex transfer of energy then takes place that results in a cloud of ions and electrons which then drift in opposite directions under the influence of an applied electric field. In commonly used gases (argon, xenon), approximately 30 eV are required for the creation of each ion pair yielding 250 electrons per 8 keV photon. Gas detectors can display several modes of operation and the simplest is that employed in ion chambers where a potential difference is applied to the electrodes to ensure efficient collection of the initial ionization. The X-ray intensity is then determined by measuring the current flow between the anode and cathode electrodes. Ion chambers are integrating detectors and the lack of any gain means that these devices are only useful for measuring relatively high flux levels.

If the electric field is raised, the energy gained by an electron during its mean free path eventually becomes sufficient to eject further electrons from atoms with which it collides thereby initiating an electron avalanche. The high electric field is traditionally produced by applying a high positive potential to fine ($<20\ \mu\text{m}$ diameter) wires and the gain of the detector is determined by the magnitude of this field. Provided that the gain is kept below saturation level, the size of the avalanche is determined by the initial amount of ionization, which is in turn a function of the amount of energy deposited by the photon. The resulting pulse is therefore proportional to the photon energy and a proportional counter is spectrally sensitive. Another very important feature of this mode of operation is that the avalanche remains localized about its initial position and is self quenching. If the potentials are increased to maximize the gain there comes a point where the UV photons emitted during the avalanche initiate further avalanches and the avalanche region will propagate along the whole anode and continue until the field is reduced. In this mode the gain is completely saturated and the size of the output signal is independent of the amount of initial ionization. Such detectors are the well known Gieger–Muller counters.

Although the initial amount of ionization is approximately ten times less than would be created in a silicon or germanium detector, the avalanche gain can be up to 10^6 . The number of electrons applied to the front-end pre-amplifier can therefore exceed 10^7 , which is enough to make the detection of individual photons with accurate timing ($\sim\text{ns}$) and position sensing (~ 1 in 1000) relatively simple. This fact, coupled with the design flexibility inherent in the gas detection system, has led to an extraordinary diversity of designs and, although most operate as photon counters, Hasegawa and co-workers in Japan have produced integrating systems capable of coping with very high input fluxes (Mochiki & Hasegawa, 1985).

Detector designs

Most proportional counters have employed electrodes with a small size in at least one dimension in order to

produce the intense fields ($>10^6\ \text{V m}^{-1}$) required to initiate avalanches. As previously mentioned, this has traditionally been achieved using fine wires but many variations have been employed, including blades (Duijn, van Eijk, Hollander & Marx, 1986), pins (Bateman, 1985) and more recently, microstrip electrodes (Oed, 1988; Angelini, Bellazzini, Brez, Massai, Raffo, Spandre & Spezziga, 1993). Parallel-plate devices (Hendrix & Lentfer, 1986; Smith, Padmore & Buksh, 1992) have also been produced where the amplification occurs in the uniform field between two parallel-plate electrodes. Large-area ($>10\ \text{cm}$ diameter) devices have, however, proved difficult to operate at high rates as they have a tendency to discharge.

A popular design for conventional multiwire gas counters for synchrotron radiation is an active region $\sim 200\ \text{mm}$ across with $10\ \mu\text{m}$ diameter anode wires on a $1\ \text{mm}$ pitch and cathode planes of somewhat thicker wires ($30\text{--}50\ \mu\text{m}$ diameter) positioned $\sim 3\text{--}10\ \text{mm}$ either side of the anode. An illustration of a conventional MWPC of this type is shown in Fig. 1.

There has recently been a great deal of work on microstrip gas chambers (MSGCs) originally introduced by Oed (1988). MSGCs use photolithographic techniques to produce an electrode structure, similar to that shown in Fig. 2 on an insulating substrate. The technique has considerable advantages over the conventional method of stringing wires, in that devices can be mass produced to very high ($0.2\ \mu\text{m}$) tolerances with very small electrode spacings. Such spacings are very desirable to limit space-charge effects caused by the build up of positive ions which have a relatively low mobility and which modify the electric field and suppress the gas gain. Unfortunately, substrate effects have led to considerable difficulties with operational stability, particularly at high flux levels (Bateman & Connolly, 1992). Various studies to determine the optimum configuration for an MSGC have been performed (Bouclier, Garabatos, Manzin, Sauli, Shekhtman & Temmel, 1993; Beckers, Bouclier, Garabatos, Million, Sauli & Shekhtman, 1994; Brons, Brückner, Heidrich, Konorov & Paul,

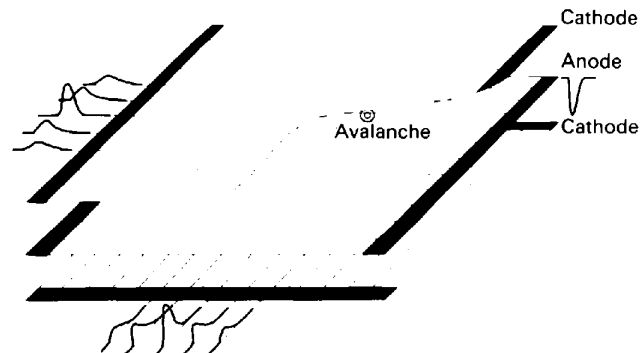


Figure 1

An MWPC configured for two-dimensional read-out showing the signals induced on the cathodes by the avalanche on the anode. Determination of the centre of gravity of the charge distribution in X and Y yields the position of the avalanche.

1993; Allunni, Bouclier, Fara, Garabatos, Manzin, Million, Ropelewski, Sauli, Shekhtman, Daubie, Pingot, Pestov, Busso & Costa, 1993; Budtz-Jorgensen, Bahnsen, Olesen, Madsen, Jonasson, Schnopper & Oed, 1991), but at the time of writing the optimum characteristics for an MSGC are still unclear with somewhat conflicting results being reported by different groups. It seems clear that the substrate must possess sufficient conductivity to prevent charge up and polarization, or gain instabilities will result; however, high-conductivity substrates can allow high current flow which causes heating. It seems almost certain that the nature of the surface of the substrate is crucial, and that differences in manufacturing techniques between groups may explain the varying results from apparently similar devices.

The Pisa group has produced devices using ion-implanted quartz to increase the surface conductivity (Angelini, Bellazzini, Brez, Massai, Spandre & Torquati, 1992). They have operated MSGCs at high pressure (Angelini, Bellazzini, Brez, Decarolis, Magazzu, Massai, Spandre, Torquati & Shekhtman, 1991) and have also developed a novel MSGC where the anodes are separated from a continuous conductive cathode by insulating strips (Angelini, Bellazzini, Brez, Massai, Raffo, Spandre & Spezziga, 1993). This device shows considerable promise as a high-rate counter with stable gains up to 8×10^6 counts $s^{-1} \text{ mm}^{-2}$.

Another recent approach is the microgap detector (Lewis, Helsby, Jones, d'Annunzio, Hall, Parker, Sumner & Worgan, 1992) which is somewhat similar to a conventional chamber and is shown in Fig. 3. It has a very much smaller ($\sim 300 \mu\text{m}$) anode-cathode spacing to minimize space-charge effects and avoids many of the difficulties caused by the substrate; however, it cannot be manufactured to such high tolerances.

Data-acquisition systems

A gas counter operated in the proportional region is both position and energy sensitive. Energy is usually determined by simply measuring the amount of charge in

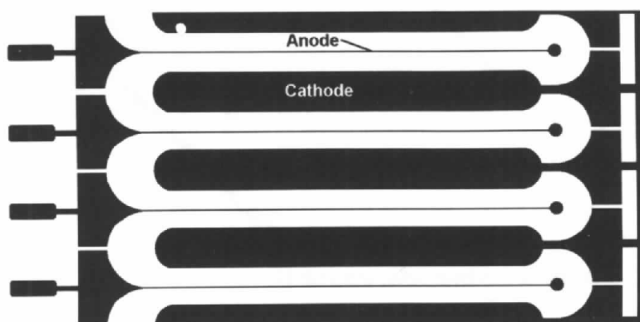


Figure 2

A typical microstrip gas detector electrode structure. Dimensions vary from device to device but typical values are $\sim 10 \mu\text{m}$ wide anodes with an anode-cathode separation of $\sim 2\text{--}300 \mu\text{m}$. The electrodes are produced using photolithography on what is usually a glass substrate.

each pulse using a charge-sensitive pre-amplifier and an analogue-digital converter (ADC). There are a variety of methods for determining the position of the X-ray photon but all rely on the fact that the avalanche remains localized about its initial position on the anode and that the charges induced on the neighbouring cathode electrodes are also localized.

The technique of charge division (Mathieson, Smith & Givin, 1980; Martin, Jelinsky, Lampton, Malina & Anger, 1981) utilizes a cathode divided into several electrodes and designed so that the amount of charge induced on each is a function of position. The actual photon position is then decoded by comparison of the signal amplitudes measured on each electrode. Whilst this technique can be very accurate, it is generally limited in speed by the difficulty of making accurate amplitude measurements quickly.

Another technique utilizes electronic delay lines (Perez-Mendez, Greenstein & Ortendahl, 1977; Gabriel & Koch, 1992; Lewis, Helsby, Jones, d'Annunzio, Hall, Parker, Sumner & Worgan, 1992) connected to two orthogonal planes of cathode wires. An avalanche causes charges to be induced on both cathodes which then pass into points along the two orthogonal delay lines. The photon interaction position is then determined by measuring the arrival times of the pulses emerging from the ends of the delay lines. This method is somewhat faster than charge division because the measurement of the time of the rising edge of the pulses is rather less susceptible to noise than the measurement of the pulse amplitude as required in charge division.

Unfortunately, both of these systems impose a rate limit on the detection system, as a second event incident upon the detector during either the charge-amplifier integration time in the case of a charge-division system, or the delay-line propagation time in a delay-line system, causes errors in the position determination. Multichannel acquisition systems can achieve higher data throughputs by handling multiple events in parallel. With the advent of cheaper processing electronics such systems are now being produced (Bateman, Connolly, Stephenson & Morse, 1992; Lewis, Fore, Helsby, Hall, Jones, Parker, Sumner & Butz-Jorgensen, 1992). The system being constructed for the Daresbury SRS utilizes an ADC connected to each electrode of the two orthogonal planes of electrodes in the microgap detector. The position is determined by the amplitudes of the signals on each wire

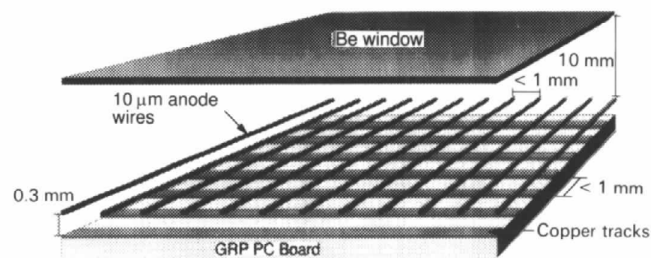


Figure 3

The microgap detector. It is similar to a conventional detector but has a greatly reduced anode-cathode gap.

and allows interpolation of the position between electrodes. It can also handle a second event elsewhere on the detector whilst another is being processed.

Operational characteristics of gas detectors

Spatial resolution

The spatial resolution of a gas detector is highly dependent upon the detector design and the associated electronics. A fundamental limit is set by the range of the primary photo electron in the gas to a few tens of micrometres for photons around 10 keV. Resolutions of 35 μm full width at half-maximum (FWHM) were obtained as long ago as 1977 (Charpak, Petersen, Policarpo & Sauli, 1978), but such high spatial resolution is not often a priority for X-ray diffraction where beam sizes are usually $>200 \mu\text{m}$ although this is likely to fall to $\sim 100 \mu\text{m}$ with the advent of more brilliant sources. In practice, the resolution is determined by signal-to-noise levels in the read-out system, and an FWHM of $\sim 1/1000$ of the size of the detector is a reasonable practical guide to what is readily achievable using non-multichannel acquisition systems. New multichannel systems will circumvent this limitation by effectively segmenting the detector into smaller read-out sections.

A typical point-spread function (PSF) of a gas detector is shown in Fig. 4, which illustrates the huge dynamic range of these devices. Such performance is only obtained for normally incident photons because the low density and finite thickness of the X-ray absorbing region leads to parallax broadening of features in the image although there are several ways to mitigate this effect. The chamber geometry can be designed with radial drift fields so that all photons scattered from a sample positioned at the focus of the field are normally incident upon a spherical detector surface. This has been used to great effect at LURE (Fourme, Bahri, Kahn & Bosshard, 1991; Kahn, Fourme, Bosshard & Saintagne, 1986). The gas pressure in the detector can be increased with a consequent decrease in the attenuation length for X-ray photons to a level which yields acceptable distortion as illustrated in Fig. 5. Another method is to use solid photocathodes so that the X-ray conversion to electrons occurs in a solid whilst the gas is used for electron multiplication; however, in their present state of development, the limited thickness of the photocathodes in such detectors tends to yield rather low detection efficiencies (Akkerman, Breskin, Chechik, Elkind, Frumkin & Gibrekhterman, 1992).

Dynamic range and signal-to-noise ratio

The dynamic range of a detector indicates the range of intensities which can be measured and is defined as the ratio between the maximum observable signal without saturation and the noise level with no illumination. It is often forgotten that the practical dynamic range of a detector cannot be divorced from its point-spread function or the type of image which it will be collecting. If the detector has a poor PSF,

a small signal in one part of the image may be swamped by the spreading of a large signal elsewhere.

Fig. 4 illustrates that features more than 2.5 mm away from a high-intensity point in the image are affected at only 10^{-4} of the peak intensity. The actual dynamic range that it is possible to record in a series of diffraction patterns is illustrated in Fig. 6.

Count rate

Perhaps the largest drawback in the use of MWPCs is that they can cope with only limited incident fluxes. The localized incident flux limit is set by space charge. MSGC and microgap technologies both use small anode-cathode separations to achieve greatly reduced space-charge limitations and stable operation at rates of $10^6 \text{ counts s}^{-1} \text{ mm}^{-2}$ are now possible as illustrated in Fig. 6.

The overall count-rate limit is normally determined by the speed of the data-acquisition system. Currently operational two-dimensional detectors such as the Daresbury

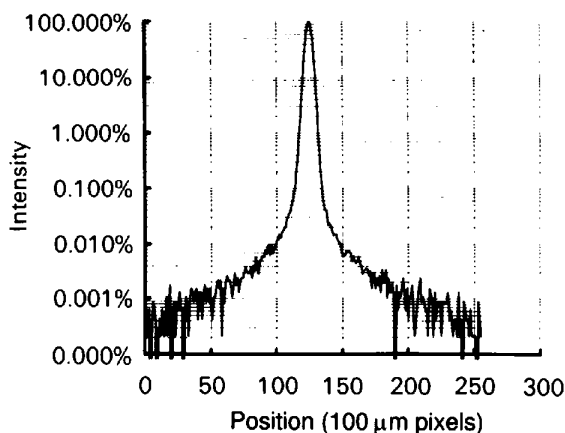


Figure 4
The point-spread function of a Daresbury delay-line gas detector for a 250 μm diameter collimated beam at normal incidence.

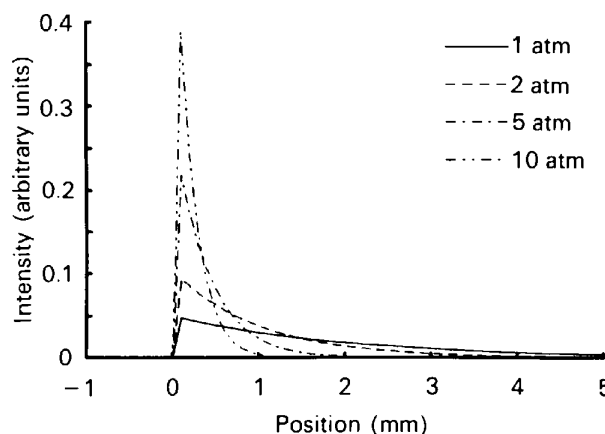


Figure 5
Illustration of the parallax broadening in a xenon-filled gas detector for photons incident at 20° from the normal to the detector for different gas pressures.

delay-line systems are limited to rates of $\sim 10^6$ counts s^{-1} but parallel read-out systems under construction (Bateman, Connolly, Stephenson & Morse, 1992; Lewis, Helsby, Jones, d'Annunzio, Hall, Parker, Sumner & Worgan, 1992) will be capable of overall rates of $\sim 2 \times 10^7$ counts s^{-1} .

Noise level

The detector noise level in a gas counter is set by the number of small discharges that are induced by spontaneous thermionic emission of electrons which subsequently cause avalanches. The number of these discharges is a strong function of the detector construction but can be kept very small. In the standard Daresbury detectors this rate plus the natural background is ~ 10 counts s^{-1} leading to a noise rate of $\sim 10^{-5}$ counts $\text{pixel}^{-1} s^{-1}$ for a 1000×1000 pixel read-out. Such a noise rate is almost always swamped by experimental background such as diffuse scatter from the sample.

Time resolution

The intrinsic time resolution of a gas detector depends upon the gas filling and geometry but existing devices can easily record data in time frames as short as $10 \mu s$. The real limitation obviously depends upon the nature of the experiment, but a limit imposed by a gas detector is its count-rate performance.

Spectral resolution

The spectral resolution obtainable from proportional counters has improved considerably with the higher manufacturing tolerances available in MSGCs. Fig. 7 shows the spectral resolution of an MSGC from a ^{241}Am source. The energy resolution in this case can be described by $\Delta E(\text{FWHM}) = 0.33[E(\text{keV})]^{0.5}$ keV which becomes comparable to that from solid-state detectors at energies below 0.5 keV.

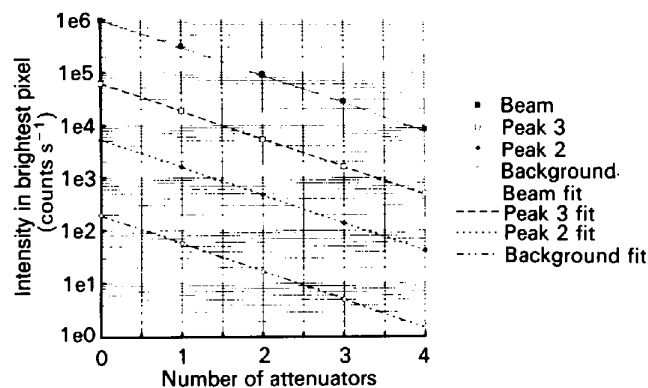


Figure 6 Illustration of the linearity of a microgap gas counter using a diffraction pattern of rat-tail collagen taken at five different count rates. The four curves relate to four different parts of the pattern having different intensities. The points are the actual data whilst the lines are a single gradient fit to all the data corrected for the different intensities. The dynamic range ($>10^6$) of the detector is clearly demonstrated.

Size and shape

Gas proportional counters have been produced in many shapes and sizes ranging from millimetres to several metres. Such flexibility means that it is possible to match the device to the type of experiment as, for example, with the curved detectors developed for high-angle diffraction (Duijn, van Eijk, Hollander & Marx, 1986; Fourme, Bahri, Kahn & Bosshard, 1991; Kahn, Fourme, Bosshard & Saintagne, 1986).

Ageing

A major difficulty with gas detectors for synchrotron radiation is that the intense fluxes can cause damage to the detectors resulting in reduced performance. In some devices such as direct-illumination CCDs, this can be extremely severe. In conventional gas detectors, ageing effects are primarily due to deposits forming on the electrodes and, depending upon the materials used in the chamber construction, they may be either conducting or insulating. Conducting deposits can increase the apparent diameter of the anode leading to reduced field and hence loss of gain, whilst insulating deposits can lead to permanent discharge effects. Various studies have been performed on the mechanisms of the deposit formation (Adam, Baird, Cockerill, Frandsen, Hilke, Hofmann, Ludlam, Rosso, Soria & Vaughan, 1983) and although the effects can be mitigated by the use of inorganic quench gases and very high gas-purity levels, operational chambers must be periodically opened and cleaned to restore their performance. Experience with the Daresbury devices shows that each device must be refurbished after approximately 3 months of use.

In MSGCs the ageing process is further complicated by the substrate and there is some evidence that these devices may be less tolerant of high flux levels than conventional chambers (Bateman & Connolly, 1992), although other devices have displayed excellent performance (Angelini, Bellazzini, Brez, Massai, Raffo, Spandre & Spezziga, 1993).

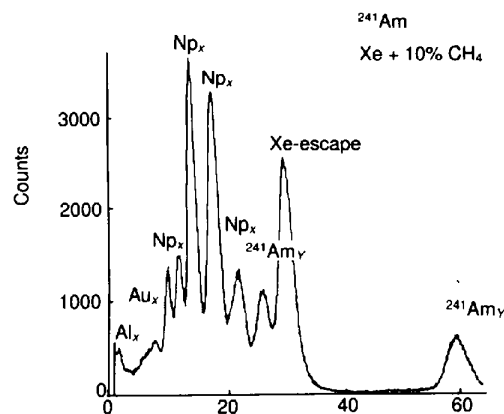


Figure 7 The energy spectrum obtained from a ^{241}Am source on a microstrip gas counter [after Budtz-Jorgensen, Bahnsen, Christensen, Muhl Madsen, Olesen & Schnopper (1992)].

Examples of gas detector performance with synchrotron radiation

Protein crystallography

Table 2 shows a comparison of the data collected from two beamlines at LURE used for protein crystallography. The W32 beamline has 50 times the intensity of D23 and is equipped with an image-plate scanner. Despite the very much higher intensity available on W32, the long read-out time of the image plate leads to a poor duty cycle and an integrated data rate which is not much higher than for the gas detector on D23. Despite the fact that image plates are excellent detectors which have been used in many successful experiments, the higher quality of the data collected on the gas detector is clearly evident from the R_{sym} values. These data demonstrate that a more intense beamline cannot always compensate for detector-performance limitations.

The signal-to-noise ratio for the gas detector is higher than that of the image plate for several reasons;

(a) The gas detector noise is negligible ($0.001 \text{ counts pixel}^{-1} \text{ s}^{-1}$ on average, *i.e.* $<1 \text{ count boxel}^{-1} \text{ frame}^{-1}$).

(b) This gas detector is larger than the image plate and hence the crystal-to-detector distance is correspondingly greater leading to a reduced background.

(c) The crystal rotation per frame, $\Delta\Phi$, is comparable with the angular width of a reflection so that the integrated background is minimal.

It should be remembered that image plates are rather less complex devices than the LURE MWPC and require far less maintenance. The most suitable detector for a given situation may therefore not simply be the one that delivers the most accurate data.

Non-crystalline diffraction

Gas detectors are routinely used for small-angle non-crystalline diffraction on the SRS, a field for which they are ideally suited because the low angles of incidence mean that parallax is not a problem. Fig. 8 shows a comparison of the

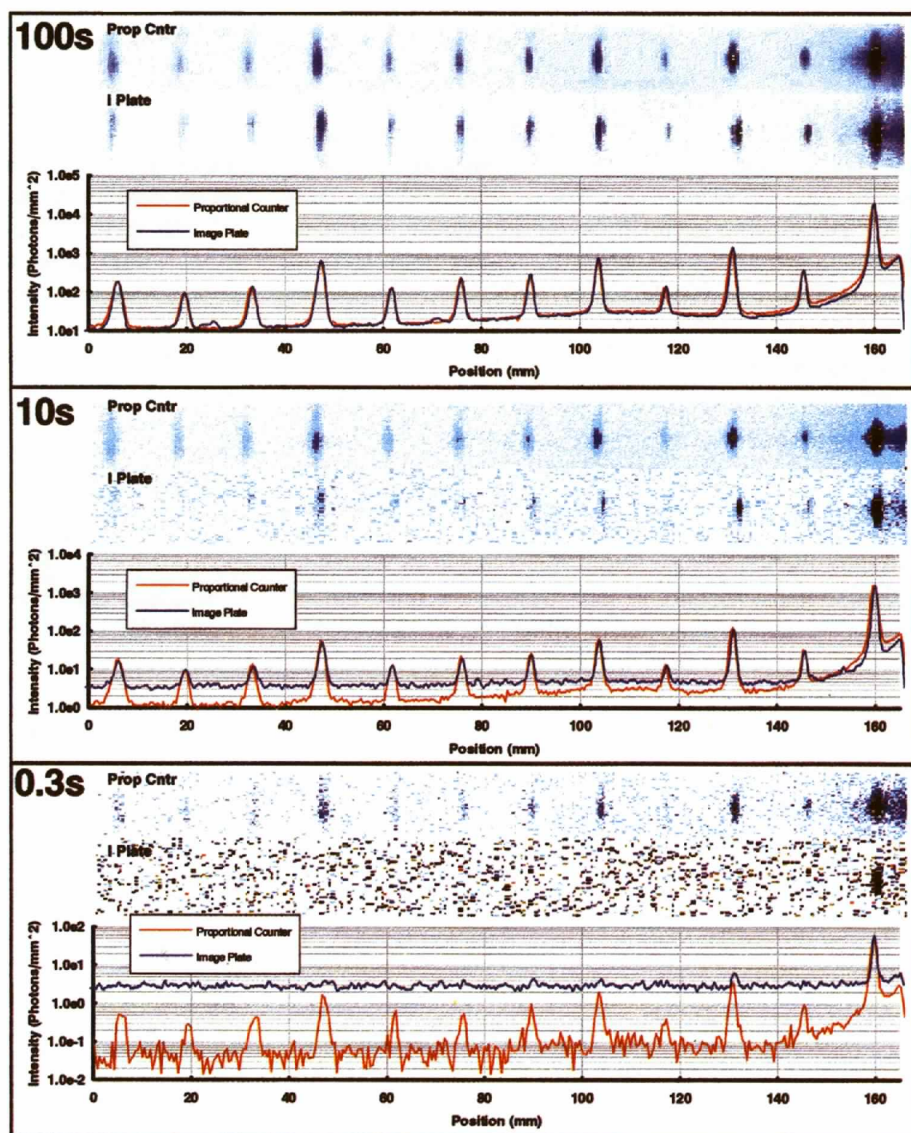


Figure 8

Three exposures of a rat-tail collagen diffraction pattern taken with an image plate and the Daresbury two-dimensional MWPC system under identical conditions. In the 100 s exposure, no significant difference can be seen between the image plate and the MWPC image but in the 10 s exposure the higher noise level of the image plate becomes apparent. In the 0.3 s exposure, almost the entire image is below the fog level of the image plate whilst the MWPC clearly reveals the diffraction pattern features.

Table 2

Comparison of two instruments for biocrystallography at LURE. One protein crystal (from the same batch) was used for each data set [after Fourme, Bahri, Kahn & Bosshard (1991)].

	W32 instrument	D23 instrument
Source	Five-pole superconducting wiggler	Bending magnet
Optics	Point focus (Si elliptical, crystal, elliptical LSM)	Line focus (Si crystals, sagittal focusing)
Wavelength	~ 1 Å	~ 1 Å
Beam intensity (arbitrary scale)	100	~ 2
Detector type	EMBL type-II image-plate scanner	Spherical drift MWPC
Geometry	Normal beam	Inclined beam
Max. global count rate	Very high (integrating)	~ 350000 s ⁻¹
Detector useful sensitivity area	Disk diameter 180 mm	Disk diameter 486 mm
Pixel size	150 × 150 μm	1 × 1 mm
Point-spread function	~ 160 μm FWHM	≤ 1 mm FWHM Gaussian
Range/pixel	65536 (ADC units)	65536 counts
Average residual noise/pixel	~ 7	~ 10 ⁻²
Dynamic range	~ 4 decades	~ 4.8 decades
Boxel size	13 × 11 pixels	5 × 5 pixels
Rotation/frame	1°	0.05°
Exposure time/frame	30 s	15 s
Elapsed time/frame	172 s	16 s
Duty cycle	0.17	0.94
Rotation rate	20.9° h ⁻¹	11.2° h ⁻¹
R _{sym} (2.2 Å data)	0.046	0.028

diffraction patterns of rat-tail collagen taken on station 2.1 of the SRS at Daresbury on a standard delay-line detector and a Molecular Dynamics image-plate scanner. The utmost care was taken to ensure the validity of these comparisons. The image plate was thoroughly erased before all exposures and kept in a light-tight cassette at all times except during loading into the scanner which was performed in a dark room. The superior sensitivity of the gas counter is obvious for the shorter exposures where the higher noise level of the image plate is visible.

Time-resolved diffraction

The kind of time resolution possible with current devices is illustrated in Fig. 9, which shows the intensity change in one of the diffraction spots from single fibres of frog muscle as they are subject to a rapid (~0.1 μs) length change. The data were collected with a time resolution of 200 μs by repeating the experiment many times and then summing the data. Improvements in data quality for this kind of experiment require both more brilliant beams and higher count-rate capability from the detector.

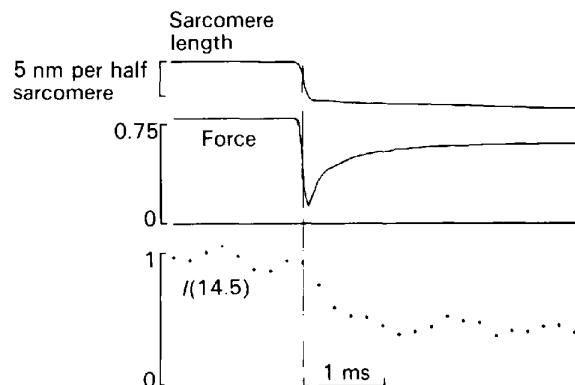
The future

As has been mentioned, the major deficiency of gas detectors for use with synchrotron radiation is their limited count-rate capability. The advent of the microstrip and microgap devices means that the count-rate bottleneck is no longer the detector but the data-acquisition systems.

Data-acquisition systems based on a single delay-line or charge-division system per axis are essentially single-channel systems, a fact which sets a fundamental limitation on possible rate performance. In these systems the *X* and *Y* coordinates of an event are associated by their proximity in time. However, as count rates are pushed to ever higher

levels, the probability of two photons impinging on the detector within a single time-resolution element increases.

The problem is illustrated in Fig. 10, which shows the probability *versus* data rate of *N* extra events occurring within 10 ns of an initial event, with *N* running from 0 to 3. It can be seen that at rates up to 10⁷ photons s⁻¹, the probability of multiple events within 10 ns is less than 0.1, but at 10⁸ photons s⁻¹ the chance of having only one event within 10 ns has fallen to 0.35. Operation at rates greater than this require either a time resolution in excess of 10 ns or, alternatively, the ability to handle simultaneous multiple events. High overall rate performance can then be achieved whilst any single channel has only to operate at modest speeds. The ultimate in this approach is the pixel detector, which has one channel, including memory, per detector pixel.

**Figure 9**

The dots in the lower trace show the change in the intensity of the 14.5 nm axial diffraction peak of single muscle fibres from the frog *Rana temporaria* when the fibre is subject to a sudden length change as shown in the top trace. The data were accumulated in 0.2 ms time frames at a wavelength of 0.15 nm on station 2.1 of the SRS [after Irving, Lombardi, Piazzesi & Ferenczi (1992)].

A highly parallel detector system is nearing completion at the SRS (Lewis, Worgan, Fore, d'Annunzio, Hall & Parker, 1991) and results from the prototype have already been published (Lewis, Fore, Helsby, Hall, Jones, Parker, Sumner & Butz-Jorgensen, 1992). Each of the 128 X and 128 Y cathodes are instrumented with a discriminator and a flash ADC. Each photon is recorded with a time resolution of <10 ns which is used to correlate the X and Y

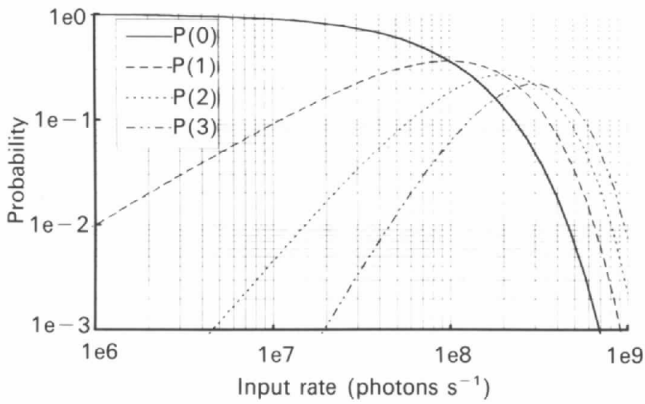


Figure 10
The probability of 0, 1, 2 and 3 events in a 10 ns time bin immediately after detection of a photon. It can be seen that at an input rate of 10^7 s^{-1} , the probability of multiple events in a bin is $\sim 10\%$. Above 10^7 s^{-1} the probability rapidly increases and therefore a photon-counting system capable of operating above this rate must be able to resolve events separated by less than 10 ns.

coordinates. The system will deliver a throughput of $>2 \times 10^7 \text{ photons s}^{-1}$ as illustrated in Fig. 12.

Fig. 11 shows two methods for handling multiple events within a single time bin. Both use semi-independent 'super-pixels' over the active area of the detector, which will allow simultaneous events to be decoded without ambiguity.

The actual performance delivered by these two systems depends upon the number of channels used, but predicted rates for 16 super-pixels or 15 diagonal wires are shown in Fig. 12. The superior performance offered by the diagonal system is due to the diagonal electrode being more independent of X and Y than the pixellated one. It therefore yields a higher information content, which ultimately allows the diagonal system to decode a much greater fraction of triple and quadruple events.

Conclusions

Synchrotron radiation sources continue to become more powerful, but it is almost inevitable that it is the very weak features at the limit of detection which must be measured at the 'cutting edge' of science. There is currently no device with the large area, low noise, good spatial resolution and very high time resolution required for these types of measurements, other than a photon-counting MWPC. The combination of the improved spectral resolution available from MSGCs coupled with the other characteristics has yet to be properly exploited within synchrotron radiation research and represents an exciting opportunity for future development.

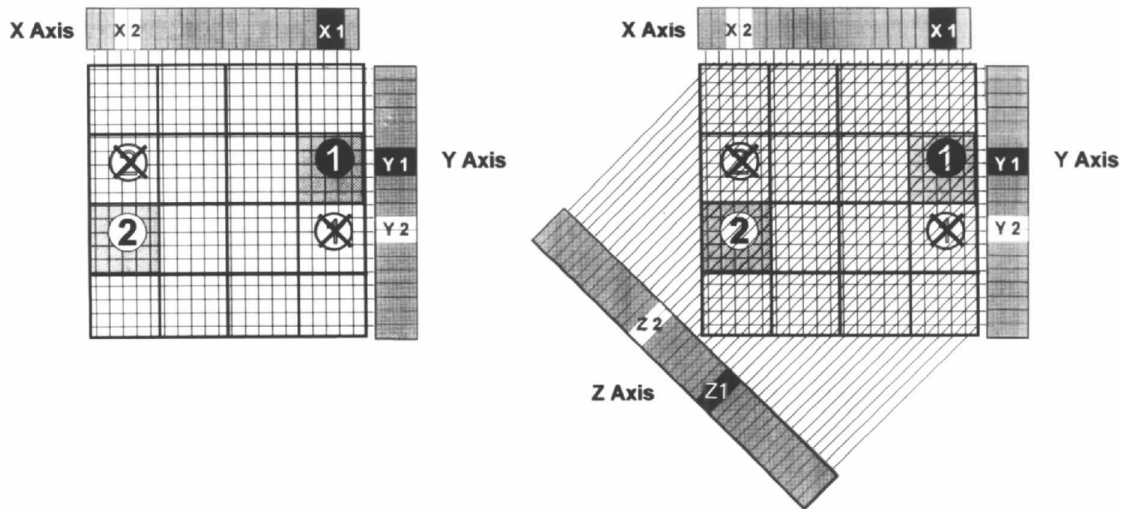


Figure 11
Two methods for improving the rate performance of a multichannel two-dimensional data-acquisition system. Consider two events 1 and 2 simultaneously incident on the detector triggering the black and white ADCs, respectively. It is impossible to unambiguously associate X1 with Y1 and X2 with Y2 in the absence of further information, leading to ambiguities at the locations marked with crosses. In the left-hand system, the detector has a pixellated electrode, and the shaded pixels would be triggered by the events 1 and 2 thereby eliminating the incorrect positions. The right-hand design uses a plane oriented at 45° to the other two which triggers the black and white diagonal ADCs marked Z1 and Z2. The resulting information can be used to correctly associate the X and Y coordinates.

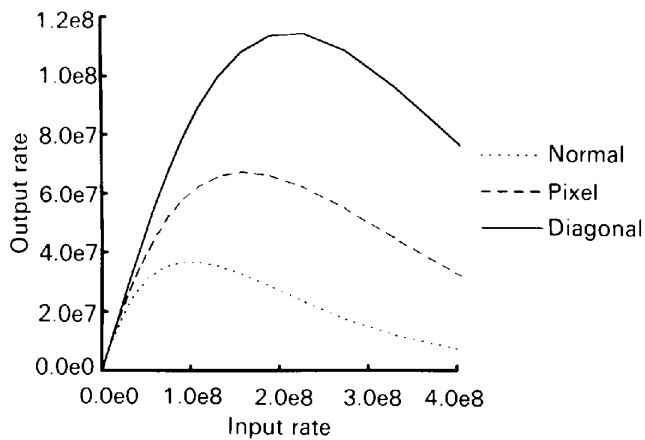


Figure 12

The predicted rate performance of perfect detectors using the normal, pixel and diagonal systems, each having a time resolution of 10 ns.

If the guideline specifications given in Table 1 are compared with the operational performance of MWPCs as described above, it is clear that many of the requirements can be readily met. The specifications which are not currently achievable are the number of pixels and the count-rate capability. Both of these deficiencies are mainly a function of the data-acquisition systems, which are presently undergoing development. The systems such as the one described above should allow detector systems that will approach the guideline requirements for diffraction in the very near future.

Despite having being written off as obsolete by those expounding the virtues of more modern devices, data continues to flow from MWPCs, leading to literally hundreds of publications each year in a wide range of scientific disciplines. Moreover, far from being a dying technology, there is vigorous development taking place on many variations of the basic MWPC in at least 20 laboratories around the world. Perhaps the recent award of the Nobel prize for Physics to G. Charpak will spur on detector developers to improve these devices still further.

References

- Adam, J., Baird, C., Cockerill, D., Frandsen, P. K., Hilke, H. J., Hofmann, H., Ludlam, T., Rosso, E., Soria, D. & Vaughan, D. (1983). *Nucl. Instrum. Methods*, **A217**, 291–297.
- Akkerman, A., Breskin, A., Chechik, R., Elkind, V., Frumkin, I. & Gibrakhterman, I. (1992). *Proceedings of the European Workshop on X-ray Detectors for Synchrotron Radiation Sources*, edited by A. H. Walenta, p. 118. Univ. of Siegen, Germany.
- Allunni, L., Bouclier, R., Fara, G., Garabatos, Ch., Manzin, G., Million, G., Ropelewski, L., Sauli, F., Shekhtman, L. I., Daubie, E., Pingot, O., Pestov, Yu. N., Busso, L. & Costa, S. (1993). Preprint CERN-PPE/93-179. CERN, Geneva, Switzerland.
- Angelini, F., Bellazzini, R., Brez, A., Decarolis, G., Magazzu, G., Massai, M. M., Spandre, G., Torquati, M. R. & Shekhtman, L. I. (1991). *Proceedings of the European Workshop on X-ray Detectors for Synchrotron Radiation Sources*, edited by A. H. Walenta, p. 96. Univ. of Siegen, Germany.
- Angelini, F., Bellazzini, R., Brez, A., Massai, M. M., Raffo, R., Spandre, G. & Spezziga, M. A. (1993). Preprint INFN PI/AE 93/10. INFN, Pisa, Italy.
- Angelini, F., Bellazzini, R., Brez, A., Massai, M. M., Spandre, G. & Torquati, M. R. (1992). *Nucl. Instrum. Methods*, **A315**, 21–32.
- Bateman, J. E. (1985). *Nucl. Instrum. Methods*, **A238**, 524–532.
- Bateman, J. E. & Connolly, J. F. (1992). Preprint RAL-92-085. Rutherford-Appleton Laboratory, Chilton, Didcot, UK.
- Bateman, J. E., Connolly, J. F., Stephenson, R. & Morse, J. (1992). *Proceedings of the European Workshop on X-ray Detectors for Synchrotron Radiation Sources*, edited by A. H. Walenta, p. 87. Univ. of Siegen, Germany.
- Beckers, T., Bouclier, R., Garabatos, Ch., Million, G., Sauli, F. & Shekhtman, L. I. (1994). Preprint CERN-PPE/94-27. CERN, Geneva, Switzerland.
- Bouclier, R., Garabatos, C., Manzin, G., Sauli, F., Shekhtman, L. & Temmel, T. (1993). Preprint CERN-PPE/93-192. CERN, Geneva, Switzerland.
- Brons, S., Brückner, W., Heidrich, M., Konorov, I. & Paul, S. (1993). Preprint CERN-PPE/93-194. CERN, Geneva, Switzerland.
- Budtz-Jorgensen, C., Bahnsen, A., Christensen, F. E., Mohl Madsen, M., Olesen, C. & Schnopper, H. W. (1992). *Proceedings of the European Workshop on X-ray Detectors for Synchrotron Radiation Sources*, edited by A. H. Walenta, p. 102. Univ. of Siegen, Germany.
- Budtz-Jorgensen, C., Bahnsen, A., Olesen, C., Madsen, M. M., Jonasson, P., Schnopper, H. W. & Oed, A. (1991). *Nucl. Instrum. Methods*, **A310**, 82–87.
- Charpak, G. (1970). *Annu. Rev. Nucl. Sci.* **20**, 195–254.
- Charpak, G., Bouclier, R., Bressani, T., Favier, J. & Zupancic, C. (1968). *Nucl. Instrum. Methods*, **62**, 202–226.
- Charpak, G., Petersen, G., Policarpo, A. & Sauli, F. (1978). *Nucl. Instrum. Methods*, **A148**, 471–482.
- Duijn, J. H., van Eijk, C. W. E., Hollander, R. W. & Marx, R. (1986). *IEEE Trans. Nucl. Sci.* **33**(1), 388–390.
- Fourme, R., Bahri, A., Kahn, R. & Bosshard, R. (1991). *Proceedings of the European Workshop on X-ray Detectors for Synchrotron Radiation Sources*, edited by A. H. Walenta, p. 16. Univ. of Siegen, Germany.
- Gabriel, A. & Koch, M. H. J. (1992). *Nucl. Instrum. Methods*, **A313**, 549–554.
- Hendrix, J. & Lentfer, A. (1986). *Nucl. Instrum. Methods*, **A252**, 246–250.
- Irving, M., Lombardi, V., Piazzesi, G. & Ferenczi, M. (1992). *Nature (London)*, **357**, 156–158.
- Kahn, R., Fourme, R., Bosshard, R. & Saintagne, V. (1986). *Nucl. Instrum. Methods*, **A246**, 596–603.
- Lewis, R. A., Fore, N. S., Helsby, W., Hall, C., Jones, A., Parker, B., Sumner, I. & Butz-Jorgensen, C. (1992). *Rev. Sci. Instrum.* **63**, 642–647.
- Lewis, R. A., Helsby, W., Jones, A., d'Annunzio, F., Hall, C., Parker, B., Sumner, I. & Worgan, J. (1992). *Proceedings of the European Workshop on X-ray Detectors for Synchrotron Radiation Sources*, edited by A. H. Walenta, pp. 61, 257. Univ. of Siegen, Germany.
- Lewis, R., Worgan, J. S., Fore, N. S., d'Annunzio, F., Hall, C. & Parker, B. (1991). *Nucl. Instrum. Methods*, **A310**, 70–73.
- Martin, C., Jelinsky, P., Lampton, M., Malina, R. F. & Anger, H. O. (1981). *Rev. Sci. Instrum.* **52**, 1067–1074.

- Mathieson, E., Smith, G. C. & Givin, P. J. (1980). *Nucl. Instrum. Methods*, **174**, 221–225.
- Mochiki, K. & Hasegawa, K. (1985). *Nucl. Instrum. Methods*, **A234**, 593–601.
- Oed, A. (1988). *Nucl. Instrum. Methods*, **A263**, 351–359.
- Perez-Mendez, V., Greenstein, M. & Ortendahl, D. (1977). *IEEE Trans. Nucl. Sci.* **24**(1), 209–212.
- Sauli, F. (1977). Report CERN 77-09. CERN, Geneva, Switzerland.
- Smith, A. D., Padmore, H. A. & Buksh, P. K. (1992). *Rev. Sci. Instrum.* **63**, 837–841.
- Walenta, A. H. (1992). *Proceedings of the European Workshop on X-ray Detectors for Synchrotron Radiation Sources*, edited by A. H. Walenta, p. 284. Univ. of Siegen, Germany.